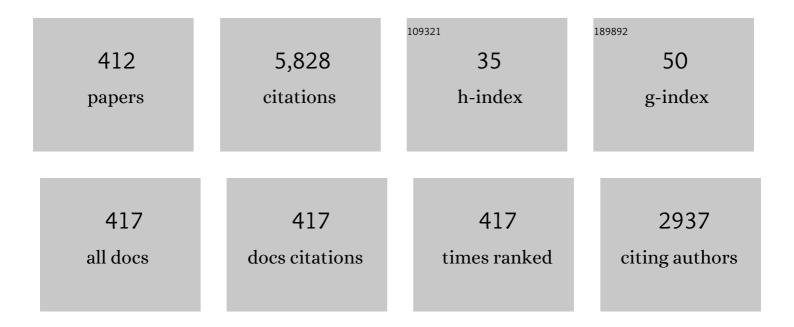
List of Publications by Year in descending order

Source: https://exaly.com/author-pdf/3556807/publications.pdf Version: 2024-02-01



#	Article	IF	CITATIONS
1	Strong convergent LP11 beam for nanoparticles trapping. Optics Communications, 2022, 503, 127446.	2.1	1
2	Spider dragline silk-based FP humidity sensor with ultra-high sensitivity. Sensors and Actuators B: Chemical, 2022, 350, 130895.	7.8	9
3	Reliability Demodulation Algorithm Design for Phase Generated Carrier Signal. IEEE Transactions on Reliability, 2022, 71, 127-138.	4.6	10
4	All-Optical Modulation Technology Based on 2D Layered Materials. Micromachines, 2022, 13, 92.	2.9	20
5	Tunable and switchable bifunctional meta-surface for plasmon-induced transparency and perfect absorption. Optical Materials Express, 2022, 12, 560.	3.0	16
6	A Temperature Sensor Based on Composite Optical Waveguide. Journal of Lightwave Technology, 2022, 40, 2663-2669.	4.6	10
7	Investigation of U-shape tapered plastic optical fibers based surface plasmon resonance sensor for RI sensing. Optik, 2022, 251, 168461.	2.9	14
8	Integrated fiber-based optoelectrode for electrochemiluminescence sensing. Optics Communications, 2022, 508, 127633.	2.1	0
9	Single Fiber Optical Tweezer for Particles Multi-Dimensional Arrangement. Journal of Lightwave Technology, 2022, 40, 1144-1149.	4.6	6
10	Intelligent all-fiber device: storage and logic computing. Photonics Research, 2022, 10, 357.	7.0	8
11	Cascaded Dual-Channel Fiber SPR Sensor Based on Ge ₂ Sb ₂ Te ₅ . IEEE Sensors Journal, 2022, 22, 4083-4089.	4.7	8
12	Bend Sensor Based on Mach-Zehnder Interferometer Using Single-Mode Fiber With Helical Structure. IEEE Photonics Technology Letters, 2022, 34, 15-18.	2.5	5
13	Dual Mode Interference Magnetic-Field Sensor Based on Hollow Suspended-Core Fiber. IEEE Photonics Technology Letters, 2022, 34, 43-46.	2.5	3
14	A Torsion Sensor Based on a Core-Deformed Long Period Fiber Grating. IEEE Photonics Technology Letters, 2022, 34, 55-58.	2.5	3
15	High Sensitivity Strain Sensor Based on Micro-Helix Micro Taper Long Period Fiber Grating. IEEE Photonics Technology Letters, 2022, 34, 432-435.	2.5	7
16	Fiber End-Facet Integrated Non-Volatile Optical Switch Based On Ge ₂ Sb ₂ Te ₅ . Journal of Lightwave Technology, 2022, 40, 3968-3973.	4.6	1
17	Investigation on the Dependence of Directional Torsion Measurement on Multimode Fiber Geometry. Journal of Lightwave Technology, 2022, 40, 3997-4002.	4.6	1
18	Design and Analysis of a Photon Counting System Using Covered Single-Photon Avalanche Photodiode. IEEE Transactions on Instrumentation and Measurement, 2022, 71, 1-9.	4.7	6

#	Article	IF	CITATIONS
19	Ultrafast metamaterial all-optical switching based on coherent modulation. Optics Express, 2022, 30, 9284.	3.4	4
20	On-Chip Photon Angular Momentum Absolute Measurement Based on Angle Detection. Nanomaterials, 2022, 12, 847.	4.1	0
21	Plastic Optical Fiber Based SPR Sensor for Simultaneous Measurement of Refractive Index and Liquid Level. IEEE Sensors Journal, 2022, 22, 6677-6684.	4.7	22
22	A highly sensitive torsion sensor based on symmetrically polished SMS fiber structure. Sensors and Actuators A: Physical, 2022, 338, 113478.	4.1	6
23	Intensity-Modulated Polymer Optical Fiber-Based Refractive Index Sensor: A Review. Sensors, 2022, 22, 81.	3.8	21
24	Fiber-integrated optical tweezers for ballistic transport and trapping yeast cells. Nanoscale, 2022, 14, 6941-6948.	5.6	8
25	Specialty optical fibers and 2D materials for sensitivity enhancement of fiber optic SPR sensors: A review. Optics and Laser Technology, 2022, 152, 108167.	4.6	39
26	A Compact Sensor Capable of Temperature, Strain, Torsion and Curvature Measuring. Journal of Lightwave Technology, 2022, 40, 4896-4902.	4.6	8
27	An Improved Strain Sensor Based on Long-Period Fiber Grating With a Local Ellipse-Core Structure. IEEE Sensors Journal, 2022, 22, 11756-11762.	4.7	2
28	Sinusoidal-Core Long Period Fiber Grating for Refractive Index Measurement. Journal of Lightwave Technology, 2022, 40, 4903-4910.	4.6	11
29	Multifunctional analysis and verification of lightning-type electromagnetic metasurfaces. Optics Express, 2022, 30, 17008.	3.4	11
30	Directional torsion sensor based on long period fiber gratings inscribed by periodically micro taper. Optical Fiber Technology, 2022, 71, 102908.	2.7	6
31	All-optical vector magnetic field sensor based on a side-polished two-core fiber Michelson interferometer. Optics Express, 2022, 30, 22746.	3.4	10
32	Temperature-Compensated Multi-Point Strain Sensing Based on Cascaded FBG and Optical FMCW Interferometry. Sensors, 2022, 22, 3970.	3.8	7
33	Integrated Multifunctional Graphene Discs 2D Plasmonic Optical Tweezers for Manipulating Nanoparticles. Nanomaterials, 2022, 12, 1769.	4.1	3
34	Optical Fiber Magnetic Field Sensor Based on Silk Fibroin Hydrogel. IEEE Sensors Journal, 2022, 22, 14878-14882.	4.7	2
35	Highly Sensitive Bending Sensor Based on Multicore Optical Fiber With Diagonal Cores Reflector at the Fiber Tip. Journal of Lightwave Technology, 2022, 40, 6030-6036.	4.6	6
36	Liquid Level Sensor With High Sensitivity Based on Hetero Core Structure. IEEE Sensors Journal, 2022, 22, 14051-14057.	4.7	3

#	Article	IF	CITATIONS
37	Long-period fiber grating humidity sensor based on spider silks. Sensors and Actuators A: Physical, 2022, 342, 113660.	4.1	4
38	Fiber Humidity Sensor Based on SF-LiBr Composite Film. IEEE Sensors Journal, 2022, 22, 16886-16891.	4.7	6
39	High-sensitivity strain sensor based on a helical-core long-period fiber grating. Optics Letters, 2022, 47, 3748.	3.3	3
40	All-fiber nonvolatile broadband optical switch using an all-optical method. Optics Letters, 2022, 47, 3604.	3.3	7
41	A dark hollow beam generator based on special optical fiber with long period fiber grating. Optics and Laser Technology, 2021, 134, 106598.	4.6	2
42	Thermal Diffusion Technique for In-Fiber Discrete Waveguide Manipulation and Modification: A Tutorial. Journal of Lightwave Technology, 2021, 39, 3638-3653.	4.6	8
43	High Accuracy Distributed Polarization Extinction Ratio Measurement For a Polarization-Maintaining Device With Strong Polarization Crosstalk. Journal of Lightwave Technology, 2021, 39, 2177-2186.	4.6	6
44	Highly Sensitive Flexible Surface Plasmon Resonance Sensor Based on Sideâ€Polishing Helicalâ€Core Fiber: Theoretical Analysis and Experimental Demonstration. Advanced Photonics Research, 2021, 2, 2000054.	3.6	6
45	A Twin-Core and Dual-Hole Fiber Design and Fabrication. Journal of Lightwave Technology, 2021, 39, 4028-4033.	4.6	4
46	Design and Fabrication of a Functional Fiber for Micro Flow Sensing. Journal of Lightwave Technology, 2021, 39, 290-294.	4.6	5
47	Rotating Angle Modulation Method for Improving the Measurement Performance of LRSPR Sensor. IEEE Sensors Journal, 2021, 21, 14876-14886.	4.7	5
48	Review of Optical Fiber Sensor Network Technology Based on White Light Interferometry. Photonic Sensors, 2021, 11, 31-44.	5.0	12
49	Photosensitive Polymer-Based Micro-Nano Long-Period Fiber Grating for Refractive Index Sensing. Journal of Lightwave Technology, 2021, 39, 6952-6957.	4.6	9
50	Parallel Polished Plastic Optical Fiber-Based SPR Sensor for Simultaneous Measurement of RI and Temperature. IEEE Transactions on Instrumentation and Measurement, 2021, 70, 1-8.	4.7	31
51	Ultra-compact Universal Linear-Optical Logic Gate Based on Single Rectangle Plasmonic Slot Nanoantenna. Plasmonics, 2021, 16, 973-980.	3.4	1
52	An All-Optical Vector Magnetic Field Sensor Based on Magnetic Fluid and Side-Polished Hollow-Core Optical Fiber. IEEE Sensors Journal, 2021, 21, 21410-21416.	4.7	19
53	High-Sensitivity Refractive Index Sensor Based on a Cascaded Core-Offset and Macrobending Single-Mode Fiber Interferometer. Frontiers in Materials, 2021, 7, .	2.4	11
54	Spider silk-based fiber magnetic field sensor. Journal of Lightwave Technology, 2021, , 1-1.	4.6	4

#	Article	IF	CITATIONS
55	Compact all-fiber thermo-optic modulator based on a Michelson interferometer coated with NaNdF ₄ nanoparticles. Optics Express, 2021, 29, 6854.	3.4	5
56	An Enhanced Plastic Optical Fiber-Based Surface Plasmon Resonance Sensor with a Double-Sided Polished Structure. Sensors, 2021, 21, 1516.	3.8	20
57	In-fiber optofluidic online SERS detection of trace uremia toxin. Optics Letters, 2021, 46, 1101.	3.3	12
58	Wide-range tunable, dual-band, background refractive index insensitive terahertz absorber based on graphene and Dirac semimetal. Optical Engineering, 2021, 60, .	1.0	3
59	Design and Analysis of an Afterpulsing Auto-Correction System for Single Photon Avalanche Diodes. IEEE Photonics Technology Letters, 2021, 33, 293-296.	2.5	5
60	High Torsion Sensitivity Sensor Based on LPFG With Unique Geometric Structure. IEEE Sensors Journal, 2021, 21, 6217-6223.	4.7	12
61	Refractive index and temperature measurement by cascading macrobending fiber and a sealed alternated SMF-MMF structure. Optics Communications, 2021, 485, 126738.	2.1	17
62	Determination of the antibiotic minocycline by integrated optofluidic microstructured polymer optical fiber chemiluminescence. Instrumentation Science and Technology, 2021, 49, 571-584.	1.8	6
63	Temperature and Refractive Index-Independent Mode Converter Based on Tapered Hole-Assisted Dual-Core Fiber. Journal of Lightwave Technology, 2021, 39, 2522-2527.	4.6	2
64	All-Fiber Hollow Bessel-Like Beam for Large-Size Particle Trap. Journal of Lightwave Technology, 2021, 39, 3291-3296.	4.6	3
65	A spiral-polished fiber sensor for strain and temperature measurement. Applied Physics B: Lasers and Optics, 2021, 127, 1.	2.2	1
66	On-chip continuous position control of phase singularities in nanoscale. Optics Express, 2021, 29, 17375.	3.4	0
67	Review of Helical Long-Period Fiber Gratings. Photonics, 2021, 8, 193.	2.0	7
68	All-fiber bidirectional optical modulator derives from the microfiber coated with ITO electrode. Optics Letters, 2021, 46, 2497.	3.3	5
69	SPR sensor based on Bessel-like beam. Optics Express, 2021, 29, 18305.	3.4	9
70	In-situ SERS detection of quinolone antibiotic residues inwater environment based on the optofluidic in-fiberintegrated Ag NPs. Applied Optics, 2021, 60, 6659-6664.	1.8	4
71	High Q-Factor Hybrid Metamaterial Waveguide Multi-Fano Resonance Sensor in the Visible Wavelength Range. Nanomaterials, 2021, 11, 1583.	4.1	14
72	Ultra-high sensitivity SPR temperature sensor based on a helical-core fiber. Optics Express, 2021, 29, 22417.	3.4	22

#	Article	IF	CITATIONS
73	Highly sensitive vector bending sensor based on an embedded multimode D-shaped LPFG. Optics Express, 2021, 29, 22813.	3.4	10
74	Distributed Polarization Measurement for Fiber Sensing Coils: A Review. Journal of Lightwave Technology, 2021, 39, 3699-3710.	4.6	13
75	A strain sensor with low temperature crosstalk based on re-modulation of D-shaped LPFG. Measurement: Journal of the International Measurement Confederation, 2021, 177, 109300.	5.0	7
76	Tunable circular dichroism based on graphene-metal split ring resonators. Optics Express, 2021, 29, 21020.	3.4	19
77	Mode division multiplexing for multiple particles noncontact simultaneous trap. Optics Letters, 2021, 46, 3017.	3.3	8
78	A Long Period Grating Sensor Based on Helical Capillary Optical Fiber. Journal of Lightwave Technology, 2021, 39, 4884-4891.	4.6	18
79	Dual-color meta-image display with a silver nanopolarizer based metasurface. Optics Express, 2021, 29, 25894.	3.4	5
80	Light-induced micro-vibrator with controllable amplitude and frequency. Optics Express, 2021, 29, 27228.	3.4	1
81	Multicore fiber integrated beam shaping devices for long-range plasmonic trapping. Optics Express, 2021, 29, 28416.	3.4	1
82	Supercontraction of spider dragline silk for humidity sensing. Optics Express, 2021, 29, 28864.	3.4	3
83	Allâ€Fiber Optical Waveform Converter Based on Deformed Catenary Nanostructure. Advanced Photonics Research, 2021, 2, 2100042.	3.6	6
84	Broadband tunable perfect absorber with high absorptivity based on double layer graphene. Optical Materials Express, 2021, 11, 3398.	3.0	10
85	Refractometer based on fiber Mach-Zehnder interferometer composed of two micro bending cores. Optics Express, 2021, 29, 31443.	3.4	12
86	Sensing Characteristics of Collapsed Long Period Fiber Gratings in Tri-Hole Fiber. Journal of Lightwave Technology, 2021, 39, 6008-6012.	4.6	8
87	Surface-Enhanced Raman Spectroscopy Detection of Cerebrospinal Fluid Glucose Based on the Optofluidic In-Fiber-Integrated Composites of Graphene Oxide, Silver Nanoparticles, and 4-Mercaptophenylboronic Acid. ACS Applied Nano Materials, 2021, 4, 10784-10790.	5.0	11
88	Simultaneous temperature and bending sensor based on Fabry-Perot interferometer with Vernier effect. Optical Fiber Technology, 2021, 66, 102657.	2.7	9
89	Measurement of liquid thermo-optical coefficient based on all-fiber hybrid FPI-SPR sensor. Sensors and Actuators A: Physical, 2021, 331, 112954.	4.1	8
90	Multifunctional fiber-optic sensor, based on helix structure and fiber Bragg gratings, for shape sensing. Optics and Laser Technology, 2021, 143, 107327.	4.6	16

#	Article	IF	CITATIONS
91	On-line SERS detection of bilirubin based on the optofluidic in-fiber integrated GO/Ag NPs for rapid diagnosis of jaundice. Talanta, 2021, 234, 122692.	5.5	4
92	Ultrasensitive Strain Sensor Based on Mach-Zehnder Interferometer With Bent Structures. Journal of Lightwave Technology, 2021, 39, 6958-6967.	4.6	14
93	Optical detection of ammonia in water using integrated up-conversion fluorescence in a fiberized microsphere. Journal of Lightwave Technology, 2021, , 1-1.	4.6	1
94	Highly Sensitive Graphene-Au Coated Plasmon Resonance PCF Sensor. Sensors, 2021, 21, 818.	3.8	33
95	Design of a Real-Time Breakdown Voltage and On-Chip Temperature Monitoring System for Single Photon Avalanche Diodes. Electronics (Switzerland), 2021, 10, 25.	3.1	2
96	All-Fiber Strain Sensor Based on Dual Side V-Grooved Long-Period Fiber Grating. IEEE Sensors Journal, 2021, 21, 21572-21576.	4.7	3
97	Fabrication and application of a novel long period fiber grating with arched fiber cores. Optical Fiber Technology, 2021, 67, 102708.	2.7	2
98	High Sensitivity Humidity Sensor Based on Side-Polished Eccentric Hole-Assisted Dual-Core Fiber. , 2021, , .		0
99	Humidity Sensor Based on Twin-Core Fiber Coated By Graphene-Oxide. , 2021, , .		0
100	Ultra-broadband perfect solar energy absorber based on tungsten ring arrays. Engineering Research Express, 2021, 3, 045020.	1.6	6
101	Simulation of On-Chip Broadband Photon Spin Router Base on Nondiffracting Surface Plasmon Beam Launching. Applied Sciences (Switzerland), 2021, 11, 10643.	2.5	4
102	Unconditionally Secure Relativistic Quantum Qubit Commitment. Applied Sciences (Switzerland), 2021, 11, 11416.	2.5	0
103	FBG Smart Bolts and Their Application in Power Grids. IEEE Transactions on Instrumentation and Measurement, 2020, 69, 2515-2521.	4.7	17
104	All-fiber phase shifter based on hollow fiber interferometer integrated with Au nanorods. Sensors and Actuators A: Physical, 2020, 301, 111750.	4.1	3
105	Double-cladding optical fiber design and optimization for simplifying the STED system. Optical Fiber Technology, 2020, 54, 102108.	2.7	2
106	High sensitivity humidity sensor based on gelatin coated side-polished in-fiber directional coupler. Sensors and Actuators B: Chemical, 2020, 305, 127555.	7.8	50
107	All-Fiber Active Tractor Beam Generator and its Application. Journal of Lightwave Technology, 2020, 38, 1420-1426.	4.6	3
108	A compact refractive index sensor with high sensitivity based on multimode interference. Sensors and Actuators A: Physical, 2020, 315, 112360.	4.1	11

#	Article	IF	CITATIONS
109	Twisted tapered plastic optical fibers for continuous liquid level sensing. Optical Fiber Technology, 2020, 59, 102318.	2.7	5
110	Ultracompact metaimage display and encryption with a silver nanopolarizer based metasurface. Applied Physics Letters, 2020, 117, 021105.	3.3	12
111	High-Sensitivity Strain and Temperature Simultaneous Measurement Sensor Based on Multimode Fiber Chirped Long-Period Grating. IEEE Sensors Journal, 2020, 20, 14843-14849.	4.7	25
112	Robust whispering gallery mode resonator for humidity measurement. Optical Fiber Technology, 2020, 60, 102378.	2.7	2
113	Graphene Oxide Sensitized No-Core Fiber Step-Index Distribution Sucrose Sensor. Photonics, 2020, 7, 101.	2.0	14
114	Torsion and Temperature Sensor Based on Polished MSM Structure. IEEE Photonics Technology Letters, 2020, 32, 1117-1120.	2.5	16
115	Ultrasensitive temperature sensor based on a urethane acrylate-coated off-axis spiral long period fiber grating. Optik, 2020, 223, 165557.	2.9	13
116	A New Sensor for Simultaneous Measurement of Strain and Temperature. IEEE Photonics Technology Letters, 2020, 32, 1253-1256.	2.5	7
117	Connecting Technologies for Coaxial Dual Core Optical Fiber. Journal of Lightwave Technology, 2020, 38, 6629-6634.	4.6	1
118	A new strain sensor based on depth-modulated long-period fiber grating. Infrared Physics and Technology, 2020, 111, 103520.	2.9	10
119	Color Variation of the Up-Conversion Luminescence in Er ³⁺ -Yb ³⁺ Co-Doped Lead Germanate Glasses and Microsphere Integrated Devices. Journal of Lightwave Technology, 2020, 38, 4397-4401.	4.6	3
120	Coherent Perfect Absorber Based on Antisymmetric Metasurface With Gain Material. IEEE Photonics Journal, 2020, 12, 1-9.	2.0	1
121	High precision roughness sensor based on annular core optical fiber. Review of Scientific Instruments, 2020, 91, 065001.	1.3	4
122	All-fiber spectral modulating device based on microfiber interferometer grown with tungsten disulfide. Instrumentation Science and Technology, 2020, 48, 505-517.	1.8	2
123	Spider Silk-Based Improved Multimode Interference Structure for Humidity Sensing. IEEE Sensors Journal, 2020, 20, 7069-7073.	4.7	5
124	Wide-range frequency tunable absorber based on cross-groove metamaterials and graphene-sheet. Journal Physics D: Applied Physics, 2020, 53, 255102.	2.8	4
125	Spider silk-based tapered optical fiber for humidity sensing based on multimode interference. Sensors and Actuators A: Physical, 2020, 313, 112179.	4.1	24
126	Investigation on the Polarization Dependence of An Angled Polished Multimode Fibre Structure. Journal of Lightwave Technology, 2020, 38, 4520-4525.	4.6	8

#	Article	IF	CITATIONS
127	A miniature ultra long period fiber grating for simultaneous measurement of axial strain and temperature. Optics and Laser Technology, 2020, 126, 106121.	4.6	42
128	A Compact Refractometer With High Sensitivity Based on Multimode Fiber Embedded Single Mode-No Core-Single Mode Fiber Structure. Journal of Lightwave Technology, 2020, 38, 1929-1935.	4.6	11
129	A Novel Twist Sensor Based on Long-Period Fiber Grating Written in Side-Helical Polished Structure. IEEE Photonics Technology Letters, 2020, 32, 275-278.	2.5	12
130	The Influence of Structural Parameters on the Surface Plasmon Resonance Sensor Based on a Side-Polished Macrobending Plastic Optical Fiber. IEEE Sensors Journal, 2020, 20, 4245-4250.	4.7	20
131	Self-Calibrated Absolute Thickness Measurement of Opaque Specimen Based on Differential White Light Interferometry. IEEE Transactions on Instrumentation and Measurement, 2020, 69, 2507-2514.	4.7	8
132	Simultaneous trapping of low-index and high-index microparticles using a single optical fiber Bessel beam. Optics and Lasers in Engineering, 2020, 131, 106119.	3.8	17
133	Simultaneous measurement of temperature and refractive index based on a hybrid surface plasmon resonance multimode interference fiber sensor. Applied Optics, 2020, 59, 1225.	1.8	38
134	Few-mode fiber-embedded long-period fiber grating for simultaneous measurement of refractive index and temperature. Applied Optics, 2020, 59, 9248.	1.8	9
135	Highly sensitive strain sensor based on a long-period fiber grating with chain-shaped structure. Applied Optics, 2020, 59, 10278.	1.8	14
136	Spin-orbital coupling of quadratic-power-exponent-phase vortex beam propagating in a uniaxial crystal. Optics Express, 2020, 28, 216.	3.4	6
137	Multi-parameter sensing based on surface plasma resonance with tungsten disulfide sheets coated. Optics Express, 2020, 28, 6084.	3.4	16
138	Pressure vector sensor based on an orthogonal optical path Sagnac interferometer. Optics Express, 2020, 28, 7969.	3.4	10
139	All fiber compact bending sensor with high sensitivity based on a multimode fiber embedded chirped long-period grating. Optics Letters, 2020, 45, 4172.	3.3	28
140	Graphene decorated twin-core fiber Michelson interferometer for all-optical phase shifter and switch. Optics Letters, 2020, 45, 177.	3.3	22
141	Laser-induced rotary micromotor with high energy conversion efficiency. Photonics Research, 2020, 8, 534.	7.0	4
142	Resolution-improved SPR sensor with a rotational modulation method. Applied Optics, 2020, 59, 2883.	1.8	10
143	Metallic structure functional sensor based on embedded PANDA fiber by ultrasonic additive manufacturing. Applied Optics, 2020, 59, 4880.	1.8	2
144	A special double-cladding fiber for generating dark hollow beam. Optik, 2020, 206, 164319.	2.9	0

#	Article	IF	CITATIONS
145	Compact fiber strain sensor fabricated by a CO ₂ laser. Optics Letters, 2020, 45, 4156.	3.3	20
146	Transmission enhanced SPR nano-microscope. Optics Express, 2020, 28, 22297.	3.4	1
147	All-fiber phase modulator and switch based on local surface plasmon resonance effect of the gold nanoparticles embedded in gel membrane. Applied Optics, 2020, 59, 10506.	1.8	4
148	Distributed Measurement of Polarization Characteristics for a Multifunctional Integrated Optical Chip: A Review. IEEE Transactions on Instrumentation and Measurement, 2019, 68, 1543-1553.	4.7	15
149	Circular Airy Beam Shaping by Annular Arrayed-Core Fiber. Journal of Lightwave Technology, 2019, 37, 4844-4850.	4.6	6
150	A special three-layer step-index fiber for building compact STED systems. Scientific Reports, 2019, 9, 8455.	3.3	6
151	An in-fiber integrated multifunctional mode converter. Optical Fiber Technology, 2019, 52, 101961.	2.7	3
152	Thin-film Thickness Absolute Measurement by Differential Optic-fiber White Light Interferometry. , 2019, , .		2
153	High-Sensitivity Plasmonics Biosensor Based on Graphene Ribbon Arrays. , 2019, , .		1
154	High Dynamic Range Photo-Detection Module Using On-Chip Dual Avalanche Photodiodes. IEEE Photonics Technology Letters, 2019, 31, 1940-1943.	2.5	4
155	A Cascade Fiber Optic Sensors for Simultaneous Measurement of Strain and Temperature. , 2019, 3, 1-4.		5
156	High sensitivity directional torsion sensor based on cascaded multimode and Mach-Zehnder interferometers with spiral structure. Engineering Research Express, 2019, 1, 025041.	1.6	0
157	Displacement Sensor Based on a Small U-Shaped Single-Mode Fiber. Sensors, 2019, 19, 2531.	3.8	18
158	A SPAD-Based Configurable Photon Counting System. IEEE Photonics Journal, 2019, 11, 1-8.	2.0	3
159	Optical Fiber Sensor for Strain Monitoring of Metallic Device Produced by Very High-Power Ultrasonic Additive Manufacturing. IEEE Sensors Journal, 2019, 19, 10680-10685.	4.7	11
160	Liquid Surface Tension and Refractive Index Sensor Based on a Side-Hole Fiber Bragg Grating. IEEE Photonics Technology Letters, 2019, 31, 947-950.	2.5	7
161	Quasi-Distributed Directional Bending Sensor Based on Fiber Bragg Gratings Array in Triangle-Four Core Fiber. IEEE Sensors Journal, 2019, 19, 10728-10735.	4.7	13
162	A New Spring-Shaped Long-Period Fiber Grating With High Strain Sensitivity. IEEE Photonics Technology Letters, 2019, 31, 1163-1166.	2.5	9

#	Article	IF	CITATIONS
163	High Sensitive Torsion Sensor Based on Cascaded Pre-Twisted Taper and Multi-Mode Fiber Sheets. IEEE Photonics Technology Letters, 2019, 31, 1588-1591.	2.5	15
164	FBG Smart Bolts and its Application in Power Grid. , 2019, , .		2
165	Directional torsion and strain discrimination based on Mach-Zehnder interferometer with off-axis twisted deformations. Optics and Laser Technology, 2019, 120, 105754.	4.6	20
166	A S-shaped long-period fiber grating with ultra-high strain sensitivity. Sensors and Actuators A: Physical, 2019, 299, 111614.	4.1	6
167	Bending sensor with parallel fiber Michelson interferometers based on Vernier-like effect. Optics and Laser Technology, 2019, 120, 105679.	4.6	43
168	Observing the Viscous Relaxation Process of Silica Optical Fiber at ~1000 °C Using Regenerated Fiber Bragg Grating. Sensors, 2019, 19, 2293.	3.8	4
169	Arc-discharge-induced off-axis spiral long period fiber gratings and their sensing characteristics. Optical Fiber Technology, 2019, 52, 101950.	2.7	20
170	2 × 2 microparticles curvilinear transport channel based on dual self-accelerating beams. Journal of Applied Physics, 2019, 125, .	2.5	2
171	Recent developments in novel silica-based optical fibers. Frontiers of Information Technology and Electronic Engineering, 2019, 20, 481-489.	2.6	5
172	Heterogeneous Double Period Array Multicore Fiber and its Application in Bragg Grating Sensor. IEEE Sensors Journal, 2019, 19, 6193-6196.	4.7	3
173	High Sensitivity Refractometer Based on a Tapered-Single Mode-No Core-Single Mode Fiber Structure. Sensors, 2019, 19, 1722.	3.8	17
174	Refractive Index Sensor Based on Twisted Tapered Plastic Optical Fibers. Photonics, 2019, 6, 40.	2.0	21
175	An integrated wavelength selective coupler based on long period grating written in twin-core fiber. Optics Communications, 2019, 445, 1-4.	2.1	5
176	Cascaded Mach–Zehnder Interferometers With Vernier Effect for Gas Pressure Sensing. IEEE Photonics Technology Letters, 2019, 31, 591-594.	2.5	28
177	Gelatin-Coated Michelson Interferometric Humidity Sensor Based on a Multicore Fiber With Helical Structure. Journal of Lightwave Technology, 2019, 37, 2452-2457.	4.6	36
178	A Highly Sensitive Torsion Sensor With a New Fabrication Method. IEEE Photonics Technology Letters, 2019, 31, 463-466.	2.5	16
179	Humidity Sensor Based on an In-Fiber Integrated Mach–Zehnder Interferometer. IEEE Photonics Technology Letters, 2019, 31, 393-396.	2.5	18
180	Optical Blade Tip-timing System Based on the Micro-structured Surface Using Phase Demodulation Algorithm. , 2019, , .		0

#	Article	IF	CITATIONS
181	High-Accuracy Distributed Polarization Crosstalk Measurements Based on White Light Interferometry. , 2019, , .		2
182	Refractive Index Sensor Based on Fiber Bragg Grating in Hollow Suspended-Core Fiber. IEEE Sensors Journal, 2019, 19, 11961-11964.	4.7	20
183	Vortex Beam Encoded All-Optical Logic Gates Based on Nano-Ring Plasmonic Antennas. Nanomaterials, 2019, 9, 1649.	4.1	5
184	Distributed Measurement of Regeneration Ratios of an Apodized Type I Fiber Bragg Grating. Journal of Lightwave Technology, 2019, 37, 6127-6132.	4.6	3
185	A novel polyvinyl alcohol and hypromellose gap-coated humidity sensor based on a Mach–Zehnder interferometer with off-axis spiral deformation. Sensors and Actuators B: Chemical, 2019, 284, 323-329.	7.8	22
186	All-optical graphene-oxide humidity sensor based on a side-polished symmetrical twin-core fiber Michelson interferometer. Sensors and Actuators B: Chemical, 2019, 284, 623-627.	7.8	70
187	Numerical simulation of coupling characteristics of optical fiber with a rectangular hole. Optical Fiber Technology, 2019, 48, 65-69.	2.7	0
188	High Strain Sensitivity Temperature Sensor Based on a Secondary Modulated Tapered Long Period Fiber Grating. IEEE Photonics Journal, 2019, 11, 1-8.	2.0	34
189	Bend-compensated long period grating in hole-assisted eccentric-core fiber. Optics Communications, 2019, 434, 19-22.	2.1	6
190	Highly Sensitive Vector Curvature Sensor Based on Two Juxtaposed Fiber Michelson Interferometers With Vernier-Like Effect. IEEE Sensors Journal, 2019, 19, 2148-2154.	4.7	48
191	Optical funnel for living cells trap. Optics Communications, 2019, 431, 196-198.	2.1	7
192	Investigation of a plastic optical fiber imprinted with V-groove structure for displacement sensing. Optical Engineering, 2019, 58, 1.	1.0	9
193	Optical attraction of strongly absorbing particles in liquids. Optics Express, 2019, 27, 12414.	3.4	15
194	In-fiber integrated high sensitivity temperature sensor based on long Fabry-Perot resonator. Optics Express, 2019, 27, 14675.	3.4	12
195	Polarization controllable generation of flat superimposed OAM states based on metasurface. Optics Express, 2019, 27, 20133.	3.4	15
196	Natural spider silk as a photonics component for humidity sensing. Optics Express, 2019, 27, 21946.	3.4	10
197	Real-time self-calibration PGC-Arctan demodulation algorithm in fiber-optic interferometric sensors. Optics Express, 2019, 27, 23593.	3.4	58
198	Refractive index sensor based on etched eccentric core few-mode fiber dual-mode interferometer. Optics Express, 2019, 27, 28104.	3.4	14

#	Article	IF	CITATIONS
199	X-typed curvilinear transport of strongly absorbing particle in a dual-beam fiber optical trap. Optics Express, 2019, 27, 33967.	3.4	3
200	Sensitivity-enhanced humidity sensor based on helix structure-assisted Mach-Zehnder interference. Optics Express, 2019, 27, 35609.	3.4	17
201	Microfiber interferometer integrated with Au nanorods for an all-fiber phase shifter and switch. Optics Letters, 2019, 44, 1092.	3.3	16
202	Spider silk-based humidity sensor. Optics Letters, 2019, 44, 2907.	3.3	24
203	Super-low-power optical trapping of a single nanoparticle. Optics Letters, 2019, 44, 5165.	3.3	16
204	Optofluidic in-fiber integrated surface-enhanced Raman spectroscopy detection based on a hollow optical fiber with a suspended core. Optics Letters, 2019, 44, 5173.	3.3	18
205	Highly sensitive vector curvature sensor based on a triple-core fiber interferometer. OSA Continuum, 2019, 2, 1953.	1.8	21
206	Optimization and experiment of a miniature multimode fiber induced-LPG refractometer. OSA Continuum, 2019, 2, 2190.	1.8	7
207	Dynamically tunable polarization-independent terahertz absorber based on bulk Dirac semimetals. OSA Continuum, 2019, 2, 2477.	1.8	7
208	Difference frequency sideband generation in semiconductors. OSA Continuum, 2019, 2, 244.	1.8	0
209	Core-independent inscription of LPGs in twin-core fiber by CO ₂ laser and coupling between LPGs. Optics Express, 2019, 27, 15786.	3.4	3
210	10.1063/1.5087001.1.,2019,,.		0
211	On-line dynamic detection in the column chromatography separation based on an optical fiber surface plasmon resonance sensor. Applied Optics, 2019, 58, 5774.	1.8	1
212	Low-temperature crosstalk and surrounding refractive index insensitive vector bending sensor based on hole-assistant dual-core fiber. Applied Optics, 2019, 58, 6597.	1.8	12
213	Ultra-long-period fiber grating cascaded to a knob-taper for simultaneous measurement of strain and temperature. Optical Review, 2018, 25, 295-300.	2.0	8
214	Discriminating Twisting Direction by Polarization Maintaining Fiber Bragg Grating. IEEE Photonics Technology Letters, 2018, 30, 654-657.	2.5	6
215	High-Accuracy PER Measurement of Integrated Optic Chip Using Orthogonal Alignment Method. IEEE Photonics Technology Letters, 2018, 30, 732-735.	2.5	0
216	In-fiber integrated gas pressure sensor based on a hollow optical fiber with two cores. Sensors and Actuators A: Physical, 2018, 272, 23-27.	4.1	27

#	Article	IF	CITATIONS
217	An Integrated Fiber Michelson Interferometer Based on Twin-Core and Side-Hole Fibers for Multiparameter Sensing. Journal of Lightwave Technology, 2018, 36, 993-997.	4.6	51
218	Directional Bending Sensor Based on a Dual Side-Hole Fiber Mach–Zehnder Interferometer. IEEE Photonics Technology Letters, 2018, 30, 375-378.	2.5	35
219	A High-Temperature Humidity Sensor Based on a Singlemode-Side Polished Multimode-Singlemode Fiber Structure. Journal of Lightwave Technology, 2018, 36, 2730-2736.	4.6	27
220	Hollow fiber SPR sensor available for microfluidic chip. Sensors and Actuators B: Chemical, 2018, 265, 211-216.	7.8	25
221	A cascade structure made by two types of gratings for simultaneous measurement of temperature and strain. Optical Fiber Technology, 2018, 42, 105-108.	2.7	21
222	Optimization of GRIN lenses coupling system for twin-core fiber interconnection with single core fibers. Optics Communications, 2018, 418, 10-15.	2.1	5
223	Mechanical Strength of Optical Fiber During the Grating Regeneration. , 2018, , .		0
224	In-Fiber Integrated Sensor Array With Embedded Weakly Reflective Joint Surface. Journal of Lightwave Technology, 2018, 36, 5663-5668.	4.6	6
225	High Sensitive Directional Twist Sensor Based on a Mach–Zehnder Interferometer. IEEE Photonics Journal, 2018, 10, 1-7.	2.0	17
226	Liquid Level Sensor Based on a V-Groove Structure Plastic Optical Fiber. Sensors, 2018, 18, 3111.	3.8	26
227	Laser-Induced Microsphere Hammer-Hit Vibration in Liquid. Physical Review Letters, 2018, 121, 133901.	7.8	19
228	Optofluidic twin-core hollow fiber interferometer for label-free sensing of the streptavidin-biotin binding. Sensors and Actuators B: Chemical, 2018, 277, 353-359.	7.8	20
229	Optical trapping and axial shifting for strongly absorbing particle with single focused TEM00 Gaussian beam. Applied Physics Letters, 2018, 113, 091101.	3.3	13
230	A Calibration Method for Large Dynamic Range White Light Interferometry Using High-Order Polarization Crosstalk. Journal of Lightwave Technology, 2018, , 1-1.	4.6	5
231	Proposed phase plate for superimposed orbital angular momentum state generation. Optics Express, 2018, 26, 14792.	3.4	16
232	In-fiber whispering-gallery mode microsphere resonator-based integrated device. Optics Letters, 2018, 43, 3961.	3.3	27
233	3-dimensional dark traps for low refractive index bio-cells using a single optical fiber Bessel beam. Optics Letters, 2018, 43, 2784.	3.3	23
234	Advances in distributed measurement of polarization characteristics for Y waveguide. , 2018, , .		1

#	Article	IF	CITATIONS
235	Multi-wavelength FBC based on thermal diffusion and phase mask techniques. Optics Communications, 2018, 427, 257-260.	2.1	2
236	Electric-arc-induced strength-controllable weak polarization mode coupling in polarization maintaining fiber. Applied Optics, 2018, 57, 6446.	1.8	2
237	Fiber In-Line Mach–Zehnder Interferometer for Gas Pressure Sensing. IEEE Sensors Journal, 2018, 18, 8012-8016.	4.7	32
238	HACF-based optical tweezers available for living cells manipulating and sterile transporting. Optics Communications, 2018, 427, 563-566.	2.1	14
239	Transmission line galloping induced dynamic strain measurement of an angle brace based power transmission tower by FBG sensors. , 2018, , .		7
240	Temperature Compensated Refractometer Based on Parallel Fiber Fabry–Pérot Interferometers. IEEE Photonics Technology Letters, 2018, 30, 1262-1265.	2.5	30
241	Characterization of Distributed Polarization-Mode Coupling for Fiber Coils. , 2018, , 1-40.		3
242	Simultaneous measurement of displacement and temperature using a PMF-based dual Mach–Zehnder interferometer. Applied Optics, 2018, 57, 9683.	1.8	8
243	Investigation of a novel SMS fiber based planar multimode waveguide and its sensing performance. Optics Express, 2018, 26, 26534.	3.4	16
244	In-fiber integrated quasi-distributed high temperature sensor array. Optics Express, 2018, 26, 34113.	3.4	10
245	Embedded whispering-gallery mode microsphere resonator in a tapered hollow annular core fiber. Photonics Research, 2018, 6, 1124.	7.0	29
246	Circular Airy beams generation by annular arrayed-core fiber. , 2018, , .		2
247	High-resolution distributed polarization crosstalk measurement for polarization maintaining fiber with considerable dispersion. Optics Express, 2018, 26, 29712.	3.4	7
248	An Overlap-Splicing-Based Cavity in FBG Sensor for the Measurement of Strain and Temperature. IEEE Photonics Technology Letters, 2017, 29, 235-238.	2.5	16
249	Fiber-Based Optical Gun for Particle Shooting. ACS Photonics, 2017, 4, 642-648.	6.6	17
250	Ultra-small and highly crystallized ZnFe ₂ O ₄ nanoparticles within double graphene networks for super-long life lithium-ion batteries. Journal of Materials Chemistry A, 2017, 5, 11188-11196.	10.3	55
251	Cascaded distributed multichannel fiber SPR sensor based on gold film thickness adjustment approach. Sensors and Actuators A: Physical, 2017, 267, 526-531.	4.1	35
252	A Humidity Sensor Based on a Singlemode-Side Polished Multimode–Singlemode Optical Fibre Structure Coated with Gelatin. Journal of Lightwave Technology, 2017, 35, 4087-4094.	4.6	61

#	Article	IF	CITATIONS
253	An improved calibration method using third order polarization mode crosstalk for optical coherence domain polarimetry. , 2017, , .		0
254	Multiple Particles 3-D Trap Based on All-Fiber Bessel Optical Probe. Journal of Lightwave Technology, 2017, 35, 3849-3853.	4.6	21
255	Symmetry evaluation for an interferometric fiber optic gyro coil utilizing a bidirectional distributed polarization measurement system. Applied Optics, 2017, 56, 5614.	1.8	5
256	Highly sensitive curvature sensor based on long period fiber grating with alternately splicing multiple single/multimode structure. Optical Fiber Technology, 2017, 37, 69-73.	2.7	13
257	Design, transform and control of optical field in discrete optical system: an example. Scientific Reports, 2017, 7, 5171.	3.3	1
258	Dual-channel surface plasmon resonance refractive index sensor based on modified hetero-core structure fiber. Optics Communications, 2017, 403, 290-295.	2.1	41
259	High-Resolution Distributed Dispersion Characterization for Polarization Maintaining Fibers Based on a Closed-Loop Measurement Framework. IEEE Photonics Journal, 2017, 9, 1-8.	2.0	5
260	Research on taper zone coupling from single-core fiber to annular-core hollow beam fiber. Optical Review, 2017, 24, 33-38.	2.0	0
261	A Temperature-Insensitive Refractive Index Sensor Based on No-Core Fiber Embedded Long Period Grating. Journal of Lightwave Technology, 2017, 35, 5391-5396.	4.6	45
262	In-Fiber M-Z Interferometer Based on Cascaded Long Period Gratings in Embedded-Core Fiber. IEEE Photonics Technology Letters, 2017, 29, 1876-1879.	2.5	19
263	High Sensitive Directional Torsion Sensor Based on a Segmented Long-Period Fiber Grating. IEEE Photonics Technology Letters, 2017, 29, 2179-2182.	2.5	21
264	Fiber-Based Helical Channels Refractive Index Sensor Available for Microfluidic Chip. IEEE Photonics Technology Letters, 2017, 29, 2087-2090.	2.5	9
265	Fiber Bragg grating sensors in hollow single- and two-core eccentric fibers. Optics Express, 2017, 25, 144.	3.4	29
266	High extinction ratio D-shaped fiber polarizers coated by a double graphene/PMMA stack. Optics Express, 2017, 25, 13278.	3.4	28
267	Optofluidic in-fiber interferometer based on hollow optical fiber with two cores. Optics Express, 2017, 25, 18205.	3.4	17
268	Measurement error analysis for polarization extinction ratio of multifunctional integrated optic chips. Applied Optics, 2017, 56, 6873.	1.8	6
269	Suppression of interference noise caused by Fresnel reflection in all-fiber white-light interferometer. Applied Optics, 2017, 56, 8732.	1.8	5
270	Range extension of the optical delay line in white light interferometry. Applied Optics, 2017, 56, 4598.	2.1	7

#	Article	IF	CITATIONS
271	In-fiber refractive index sensor based on single eccentric hole-assisted dual-core fiber. Optics Letters, 2017, 42, 4470.	3.3	28
272	A Stable Twin-Core-Fiber-Based Integrated Coupler Fabricated by Thermally Diffused Core Technique. Journal of Lightwave Technology, 2017, 35, 5473-5478.	4.6	15
273	Whispering gallery mode temperature sensor of liquid microresonastor. Optics Letters, 2016, 41, 4649.	3.3	54
274	High-Order Interference Effect Introduced by Polarization Mode Coupling in Polarization—Maintaining Fiber and Its Identification. Sensors, 2016, 16, 419.	3.8	5
275	Dynamic range beyond 100 dB for polarization mode coupling measurement based on white light interferometer. Optics Express, 2016, 24, 16247.	3.4	17
276	A novel Michelson Fabry–Perot hybrid interference sensor based on the micro-structured fiber. Optics Communications, 2016, 374, 58-63.	2.1	26
277	Single fiber optical trapping of a liquid droplet and its application in microresonator. Optics Communications, 2016, 381, 371-376.	2.1	9
278	Highly Sensitive Directional Bending Sensor Based on Eccentric Core Fiber Mach–Zehnder Modal Interferometer. IEEE Sensors Journal, 2016, 16, 6899-6902.	4.7	32
279	Modal Interferometer Using Three-Core Fiber for Simultaneous Measurement Strain and Temperature. IEEE Photonics Journal, 2016, 8, 1-8.	2.0	18
280	Single-fiber tweezers applied for dye lasing in a fluid droplet. Optics Letters, 2016, 41, 2966.	3.3	16
281	Ce3+/Yb3+/Er3+ triply doped bismuth borosilicate glass: a potential fiber material for broadband near-infrared fiber amplifiers. Scientific Reports, 2016, 6, 33865.	3.3	37
282	Pure Directional Bending Measurement With a Fiber Bragg Grating at the Connection Joint of Eccentric-Core and Single-Mode Fibers. Journal of Lightwave Technology, 2016, 34, 3288-3292.	4.6	56
283	Simultaneous measurement of temperature and strain using a long-period fiber grating with a micro-taper. Optical Review, 2016, 23, 657-661.	2.0	8
284	Combining Two Types of Gratings for Simultaneous Strain and Temperature Measurement. IEEE Photonics Technology Letters, 2016, 28, 477-480.	2.5	50
285	Two-Axis Bending Sensor Based on Cascaded Eccentric Core Fiber Bragg Gratings. IEEE Photonics Technology Letters, 2016, 28, 1237-1240.	2.5	55
286	Annular arrayed-waveguide fiber for autofocusing Airy-like beams. Optics Letters, 2016, 41, 824.	3.3	17
287	Inconsistency measurement between two branches of LiNbO3 integrated optic Y-junction. Optics Communications, 2016, 369, 152-158.	2.1	7
288	Investigation of Particle Harmonic Oscillation Using Four-Core Fiber Integrated Twin-Tweezers. IEEE Photonics Technology Letters, 2016, 28, 461-464.	2.5	6

#	Article	IF	CITATIONS
289	Quasi-distributed birefringence dispersion measurement for polarization maintain device with high accuracy based on white light interferometry. Optics Express, 2016, 24, 1587.	3.4	19
290	Single optical tweezers based on elliptical core fiber. Optics Communications, 2016, 365, 103-107.	2.1	19
291	Dual-truncated-cone structure for quasi-distributed multichannel fiber surface plasmon resonance sensor. Optics Letters, 2016, 41, 4320.	3.3	13
292	Long period fiber grating in two-core hollow eccentric fiber. Optics Express, 2015, 23, 33378.	3.4	25
293	Building a lab-in/on-fiber. , 2015, , .		1
294	A mode-division-multiplexing single fiber optical tweezers. Proceedings of SPIE, 2015, , .	0.8	0
295	Single mode fiber and twin-core fiber connection technique for in-fiber integrated interferometer. , 2015, , .		1
296	Spectrum zooming in network topology based on a white light fiber optic Mach-Zehnder interferometer. Proceedings of SPIE, 2015, , .	0.8	0
297	A novel single fiber optical tweezers based on light-induced thermal effect. , 2015, , .		0
298	Highly Focused Conical Optical Field for Pico-Newton Scale Force Sensing. Journal of Lightwave Technology, 2015, 33, 2486-2491.	4.6	5
299	An improved PGC demodulation method to extend dynamic range and compensate low-frequency drift of modulation depth. , 2015, , .		3
300	A micro-particle launching apparatus based on mode-division-multiplexing technology. Optics Communications, 2015, 342, 30-35.	2.1	6
301	Graphene-Coated Surface Core Fiber Polarizer. Journal of Lightwave Technology, 2015, 33, 349-353.	4.6	39
302	A phase-shifted long period fiber grating based on filament heating method for simultaneous measurement of strain and temperature. Journal of Optics (United Kingdom), 2015, 17, 075801.	2.2	26
303	Micro particle launcher/cleaner based on optical trapping technology. Optics Express, 2015, 23, 8650.	3.4	7
304	Twin-core fiber SPR sensor. Optics Letters, 2015, 40, 2826.	3.3	71
305	Simultaneous evaluation of two branches of a multifunctional integrated optic chip with an ultra-simple dual-channel configuration. Photonics Research, 2015, 3, 115.	7.0	10
306	In-Line Mach–Zehnder Interferometric Sensor Based on a Linear Five-Core Fiber. IEEE Photonics Technology Letters, 2015, 27, 635-638.	2.5	34

#	Article	IF	CITATIONS
307	Bending characteristics of a long-period fiber grating in a hollow eccentric optical fiber. Applied Optics, 2015, 54, 7879.	2.1	20
308	An improved fixed phased demodulation method combined with phase generated carrier (PGC) and ellipse fitting algorithm. , 2015, , .		5
309	A study of multi-trapping of tapered-tip single fiber optical tweezers. Chinese Physics B, 2014, 23, 088702.	1.4	5
310	Full Evaluation of Polarization Characteristics of Multifunctional Integrated Optic Chip With High Accuracy. Journal of Lightwave Technology, 2014, 32, 4243-4252.	4.6	18
311	All-fiber self-accelerating Bessel-like beam generator and its application. Optics Letters, 2014, 39, 6185.	3.3	8
312	Compact all-fiber plasmonic Airy-like beam generator. Optics Letters, 2014, 39, 1113.	3.3	23
313	Refractive Index Sensing Characteristics of Single-Mode Fiber-Based Modal Interferometers. Journal of Lightwave Technology, 2014, 32, 1734-1740.	4.6	27
314	A Novel Temperature Sensor Based on Optical Trapping Technology. Journal of Lightwave Technology, 2014, 32, 1394-1398.	4.6	14
315	Multi-Dimensional Manipulation of Yeast Cells Using a LP\$_{11}\$ Mode Beam. Journal of Lightwave Technology, 2014, 32, 1098-1103.	4.6	18
316	An in-fiber integrated optofluidic device based on an optical fiber with an inner core. Lab on A Chip, 2014, 14, 2090.	6.0	14
317	Simultaneous Measurement of Temperature and Curvature Based on Hollow Annular Core Fiber. IEEE Photonics Technology Letters, 2014, 26, 1128-1131.	2.5	30
318	Hybrid structured fiber-optic Fabry–Perot interferometer for simultaneous measurement of strain and temperature. Optics Letters, 2014, 39, 5267.	3.3	115
319	Airy-like beam transverse acceleration control by rainbow effect. Optics Letters, 2014, 39, 1089.	3.3	7
320	Design and fabrication of a novel core-suspended optic fiber for distributed gas sensor. Photonic Sensors, 2014, 4, 97-101.	5.0	1
321	A capillary optical fiber modulator derivates from magnetic fluid. Optics Communications, 2013, 304, 83-86.	2.1	11
322	Coaxial Step index large mode area fiber with low propagation loss. , 2013, , .		0
323	Birefringence properties analysis of a novel three quasi-rectangular cores fiber. , 2013, , .		1
324	A real non-contact remote trapping single fiber tweezers. , 2013, , .		0

#	Article	IF	CITATIONS
325	Long period fiber grating and high sensitivity refractive index sensor based on hollow eccentric optical fiber. Sensors and Actuators B: Chemical, 2013, 188, 768-771.	7.8	43
326	Microfluidic in-fiber oxygen sensor derivates from a capillary optical fiber with a ring-shaped waveguide. Sensors and Actuators B: Chemical, 2013, 182, 571-575.	7.8	19
327	Mode division multiplexing technology for single-fiber optical trapping axial-position adjustment. Optics Letters, 2013, 38, 2617.	3.3	38
328	Generation of Airy-like wave with one-dimensional waveguide array. Optics Letters, 2013, 38, 1645.	3.3	17
329	Two-dimensional Airy-like beam generation by coupling waveguides. Journal of the Optical Society of America A: Optics and Image Science, and Vision, 2013, 30, 1404.	1.5	14
330	In-fiber integrated optic devices for sensing applications. Proceedings of SPIE, 2012, , .	0.8	0
331	A new real non-invasive single fiber tweezers. Proceedings of SPIE, 2012, , .	0.8	4
332	A wavelength division multiplexer based on a cocentric core fiber. , 2012, , .		1
333	A non-contact single optical fiber multi-optical tweezers probe: Design and fabrication. Optics Communications, 2012, 285, 4068-4071.	2.1	37
334	Four-Core Optical Fiber Micro-Hand. Journal of Lightwave Technology, 2012, 30, 1487-1491.	4.6	23
335	Multi-Array Sensors Tree Network Based on White Light Fiber-Optic Mach-Zehnder Interferometer. Sensor Letters, 2012, 10, 1378-1381.	0.4	2
336	Loss characteristics of helical-core fiber. Optoelectronics Letters, 2012, 8, 280-283.	0.8	1
337	An Annular Core Single Fiber Tweezers. Sensor Letters, 2012, 10, 1374-1377.	0.4	2
338	A Novel Multiplexed Fiber Optic Deformation Sensing Scheme. Sensor Letters, 2012, 10, 1526-1528.	0.4	2
339	Asymmetrical Twin-Core Fiber Based Michelson Interferometer for Refractive Index Sensing. Journal of Lightwave Technology, 2011, 29, 2985-2991.	4.6	38
340	Characteristics of Near-Surface-Core Optical Fibers. Journal of Lightwave Technology, 2011, 29, 3004-3008.	4.6	16
341	Embedded multicore hollow fiber with high birefringence. Applied Optics, 2011, 50, 6162.	2.1	6
342	Characteristics of embedded-core hollow optical fiber. Optics Express, 2011, 19, 20069.	3.4	11

#	Article	IF	CITATIONS
343	In-fiber integrated accelerometer. Optics Letters, 2011, 36, 2056.	3.3	49
344	Integrated fiber Michelson interferometer based on poled hollow twin-core fiber. Optics Letters, 2011, 36, 2435.	3.3	18
345	Optical refractometer based on an asymmetrical twin-core fiber Michelson interferometer. Optics Letters, 2011, 36, 3221.	3.3	22
346	Higher-order interference of low-coherence optical fiber sensors. Optics Letters, 2011, 36, 3380.	3.3	5
347	Mode field analysis of eccentric optical fibers by conformal mapping. , 2011, , .		4
348	Recent progress of in-fiber integrated interferometers. Photonic Sensors, 2011, 1, 1-5.	5.0	9
349	Loop topology based white light interferometric fiber optic sensor network for application of perimeter security. Photonic Sensors, 2011, 1, 260-267.	5.0	20
350	Single-polarization photonic crystal fibers with a multiplex structure. Optoelectronics Letters, 2011, 7, 57-60.	0.8	0
351	Recent progress of linkage methodology between single mode fiber and index guided microstructured fiber. Proceedings of SPIE, 2010, , .	0.8	0
352	Tunable optical-path correlator for distributed strain or temperature-sensing application. Optics Letters, 2010, 35, 3357.	3.3	14
353	Photonic Crystal Heterostructure Composed of Triangular and Honeycomb Lattice. , 2009, , .		0
354	Multiplexed Fiber Optic Twin-sensor Array based on a Combination of Mach-Zehnder and Michelson Interferometers. Journal of Intelligent Material Systems and Structures, 2009, 20, 809-813.	2.5	6
355	Fabricating of silver and copper nano/microtubes using nano-scale glass fibers as templates. Journal of Materials Science, 2009, 44, 3382-3386.	3.7	6
356	Photonic band gap of 2D complex lattice photonic crystal. Optoelectronics Letters, 2009, 5, 120-123.	0.8	5
357	Package and installation of embeddable fiber optic sensors. Optics and Lasers in Engineering, 2009, 47, 1085-1090.	3.8	8
358	Linear-core-array microstructured fiber. Optics Letters, 2009, 34, 1531.	3.3	4
359	Coupling Theoretical Model Between Single-Core Fiber and Twin-Core Fiber. Journal of Lightwave Technology, 2009, 27, 5235-5239.	4.6	22
360	Supermodes Analysis for Linear-Core-Array Microstructured Fiber. Journal of Lightwave Technology, 2009, 27, 1741-1745.	4.6	11

#	Article	IF	CITATIONS
361	FBG Sensor Demodulated by Multimode Interference of Multimode Fiber. , 2009, , .		0
362	Capillary optical fiber linking approach for biosensors. , 2009, , .		2
363	Channeled spectral interferometer based fiber optic bending sensor. Proceedings of SPIE, 2009, , .	0.8	0
364	Recent progress of multi-core fiber based integrated interferometers. Proceedings of SPIE, 2009, , .	0.8	4
365	Four-core fiber-based bending sensor. Frontiers of Optoelectronics in China, 2008, 1, 231-236.	0.2	5
366	Three-core fiber-based shape-sensing application. Optics Letters, 2008, 33, 578.	3.3	25
367	Tunable Fabry–Perot-resonator-based fiber-optic white-light interferometric sensor array. Optics Letters, 2008, 33, 1780.	3.3	6
368	Bitapered fiber coupling characteristics between single-mode single-core fiber and single-mode multicore fiber. Applied Optics, 2008, 47, 3307.	2.1	35
369	Twin-core fiber optical tweezers. Optics Express, 2008, 16, 4559.	3.4	86
370	A Compact Fiber-Optic Flow Velocity Sensor Based on a Twin-Core Fiber Michelson Interferometer. IEEE Sensors Journal, 2008, 8, 1114-1117.	4.7	72
371	Twin-core fiber white light interferometric bending sensor. , 2008, , .		2
372	Two-beam optical tweezers built by a two-core fiber. Proceedings of SPIE, 2008, , .	0.8	0
373	Three-core fiber far field structured light pattern generator and its shape sensing application. Proceedings of SPIE, 2008, , .	0.8	1
374	A fibre-optic low-coherence quasi-distributed strain sensing system with multi-configurations. Measurement Science and Technology, 2007, 18, 2931-2937.	2.6	3
375	Improving the reliability of multiplexed fiber optic low-coherence interferometric sensors by use of novel twin-loop network topologies. Review of Scientific Instruments, 2007, 78, 055106.	1.3	7
376	Interaction Model for a Hi-Bi Fiber Optic Ultrasonic Sensor and the Host Material. Journal of Intelligent Material Systems and Structures, 2007, 18, 875-878.	2.5	1
377	A novel in-fiber optical switch based on two-core optical fiber. , 2007, , .		2
378	Four-beam single fiber optic interferometer and its sensing characteristics. Sensors and Actuators A: Physical, 2007, 138, 9-15.	4.1	23

#	Article	IF	CITATIONS
379	In-fiber integrated Michelson interferometer. Optics Letters, 2006, 31, 2692.	3.3	84
380	Coupling characteristics between single-core fiber and multicore fiber. Optics Letters, 2006, 31, 3237.	3.3	54
381	Tapered fiber optical tweezers for microscopic particle trapping: fabrication and application. Optics Express, 2006, 14, 12510.	3.4	208
382	Theoretical and experimental study on white light interferometric sensing network with double-ring topology. Frontiers of Electrical and Electronic Engineering in China: Selected Publications From Chinese Universities, 2006, 1, 234-238.	0.6	1
383	Detection of acoustic emission in structure using Sagnac-like fiber-loop interferometer. Sensors and Actuators A: Physical, 2005, 118, 6-13.	4.1	29
384	Two-loop-based low-coherence multiplexing fiber-optic sensor network with a Michelson optical path demodulator. Optics Letters, 2005, 30, 601.	3.3	19
385	Schemes of a fiber-optic multiplexing sensor array based on a 3×3 star coupler. Optics Letters, 2005, 30, 961.	3.3	7
386	Loop Topology Based White Light Interferometric Fiber Optic Sensors Network. , 2005, , 463-472.		0
387	Push–pull fiber optic inclinometer based on a Mach–Zehnder optical low-coherence reflectometor. Review of Scientific Instruments, 2004, 75, 2013-2015.	1.3	4
388	Long-gauge length embedded fiber optic ultrasonic sensor for large-scale concrete structures. Optics and Laser Technology, 2004, 36, 11-17.	4.6	17
389	Low-coherence Michelson interferometric fiber-optic multiplexed strain sensor array: a minimum configuration. Applied Optics, 2004, 43, 3211.	2.1	9
390	Effect of thermally induced strain on optical fiber sensors embedded in cement-based composites. Optical Fiber Technology, 2003, 9, 95-106.	2.7	8
391	Enhancement of multiplexing capability of low-coherence interferometric fiber sensor array by use of a loop topology. Journal of Lightwave Technology, 2003, 21, 1313-1319.	4.6	12
392	Modified Michelson fiber-optic interferometer: A remote low-coherence distributed strain sensor array. Review of Scientific Instruments, 2003, 74, 270-272.	1.3	1
393	Low-coherence fiber-optic sensor ring network based on a Mach–Zehnder interrogator. Optics Letters, 2002, 27, 894.	3.3	17
394	Multiplexed, white-light interferometric fiber-optic sensor matrix with a long-cavity, Fabry-Perot resonator. Applied Optics, 2002, 41, 4460.	2.1	4
395	Design of a fiber-optic quasi-distributed strain sensors ring network based on a white-light interferometric multiplexing technique. Applied Optics, 2002, 41, 7205.	2.1	11
396	Multiplexing of fiber-optic white light interferometric sensors using a ring resonator. Journal of Lightwave Technology, 2002, 20, 1471-1477.	4.6	3

#	Article	IF	CITATIONS
397	Enhanced multiplexing capacity of low-coherence reflectometric sensors with a loop topology. IEEE Photonics Technology Letters, 2002, 14, 1157-1159.	2.5	13
398	Investigation of a coated optical fiber strain sensor embedded in a linear strain matrix material. Optics and Lasers in Engineering, 2001, 35, 251-260.	3.8	17
399	The temperature characteristic of fiber-optic pre-embedded concrete bar sensor. Sensors and Actuators A: Physical, 2001, 93, 206-213.	4.1	9
400	Fiber optic temperature sensor with duplex Michleson interferometric technique. Sensors and Actuators A: Physical, 2000, 86, 2-7.	4.1	18
401	Recent progress of white light interferometric fiberoptic strain sensing techniques. Review of Scientific Instruments, 2000, 71, 4648.	1.3	19
402	Quasi-distributed strain sensing with white-light interferometry: a novel approach. Optics Letters, 2000, 25, 1074.	3.3	45
403	Fiber-optic Moiré Interference Principle. Optical Fiber Technology, 1998, 4, 224-232.	2.7	7
404	Optical path automatic compensation low-coherence interferometric fibre-optic temperature sensor. Optics and Laser Technology, 1998, 30, 33-38.	4.6	18
405	Sensitivity coefficient evaluation of an embedded fiber-optic strain sensor. Sensors and Actuators A: Physical, 1998, 69, 5-11.	4.1	36
406	1 × N star coupler as a distributed fiber-optic strain sensor in a white-light interferometer. Applied Optics, 1998, 37, 4168.	2.1	31
407	Embedded white light interferometer fibre optic strain sensor for monitoring crack-tip opening in concrete beams. Measurement Science and Technology, 1998, 9, 261-266.	2.6	36
408	White-light interferometric fiber-optic strain sensor from three-peak-wavelength broadband LED source. Applied Optics, 1997, 36, 6246.	2.1	24
409	White-light interferometric fiber-optic distributed strain-sensing system. Sensors and Actuators A: Physical, 1997, 63, 177-181.	4.1	50
410	Enhanced multiplexing capacity of low-coherence reflectometric sensors based on a loop topology. , 0, , .		0
411	Two-channel inclinometer based on low-coherence fiber-optic Mach-Zehnder interrogation technique. , 0, , .		0
412	Ammonia Detection by Dye Immobilized Microstructured Optical Fiber. Advanced Materials Research, 0, 255-260, 2131-2135.	0.3	1